



Investigation of the Strength of Cold-Formed Steel C-Section in Compression

Arvin Patrick Yu¹, Dr. Bernardo A. Lejano²

¹ BS-MS Civil Engineering Student, De La Salle University

² Associate Professor, Civil Engineering Department, De La Salle University
bernardo.lejano@dlsu.edu.ph

Abstract: Cold-Formed Steel (CFS) may be considered as one of the excellent construction materials because it exhibits efficient load carrying capabilities in combination with its lightweight characteristics. However, there is a dearth of knowledge about the structural performance of locally-produced CFS in the Philippines and yet it is used for structures by just simply following foreign standards and guides. The objective of this study is to verify experimentally and computationally the performance of C-shaped Cold-Formed Steel (CFS) when subjected to concentric axial compression load considering buckling. The experimental aspect subjects the CFS members with compressive loads using hydraulic jacks and load cell. For the computational aspect, provisions found in the NSCP were used to determine the strength in compression of the members based on the actual dimensions, thicknesses and lengths of the member together with the material properties of the steel. This was done to a total of 126 samples with 1 section shape, 6 different lengths and 5 different thicknesses. It was found that the strength calculations for both distortional buckling failure and torsional-flexural buckling failure given by the NSCP provisions were not consistent with the results of the compression tests. For shorter lengths, distortional buckling prevailed as the main failure while for longer lengths, torsional-flexural buckling occurred. All of the predicted strength were highly conservative and well below the experimental value.

Key Words: Cold-Formed Steel; Compression Members; Light-gage steel channel

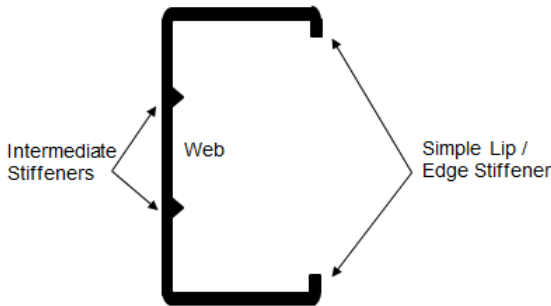
1. INTRODUCTION

There is dearth of technical information about Cold-Formed Steel (CFS) C-section locally manufactured in the Philippines and yet it is used for structures in accordance with foreign standards and guides as to how to apply CFS members. Structurally, a building must be properly analysed

and designed to withstand certain design loads and conditions. In line with it, calculations are made to evaluate the capacities of sections and members to determine if the structural elements can be used or not. In recent years, cold formed steel application for structural purposes have increased here and abroad. Davies (2000) has reviewed the advancement of CFS in terms of material quality, section properties, interaction of failures, and the widening scope of

application. Mostly, it is used as residential and low-rise buildings construction in the United States. Rondal (2000) backed up this claim and further stated that cold-formed steel members have reached the “age of maturity”.

This study focuses on understanding the accuracy of the NSCP provisions to strength determination of CFS C-sections in compression. Apparently, the existing provisions in the NSCP are based also from the standards from foreign country. The values computed using the code is not known to be greater or lesser than the true strength of the members manufactured in the Philippines. The American Iron and Steel Institute (AISI) code provisions are constantly being checked by researchers/engineers to determine the accuracy of formulas stipulated in the code and actual results from experiments. A study by Chou, Seah, & Rhodes (1996) summarized past studies’ results for cold-



formed columns and described the accuracy of the provisions used, including AISI, to the respective results of the tests. They found out similarities and differences of the calculated strength with those attained through experiments.

The main objective of this study is to verify the performance of C-shaped cold-formed steel in axial compression load with the use of experimental method and computational method. Five different thicknesses of the CFS were considered to provide a means of analysing of the effects of changing cross section parameters to the compressive strength. The typical cross-section of the C-shaped CFS is shown in Figure 1. Lengths were also changed to allow various modes of buckling failure to occur.

Fig. 1. Cross-section of the C-shaped CFS

2. METHODOLOGY

The research was categorized into two major parts, experimental and computational. The computational objective of the study was to determine through the provisions stated in the NSCP the strength of C-shaped CFS members in compression. The experimental objective was to record the strength manifested by doing compression tests on C-shaped CFS members and identifying the mode of failure. With this, the results from the two objectives were compared to one another and conclusions and trends were made.

For the computational objective, given the actual values of sizes, dimensions, thicknesses and lengths of the member together with the material properties of the steel, formulas used in the NSCP as shown in the earlier section was used to determine the strength in compression of the members. The failure modes stated in the NSCP were considered. The lowest calculated value of strength governs the strength of the member.

The experimental procedure simply subjected the CFS members to concentric compressive load with the use an improvised experimental setup using hydraulic jack, load cells, and loading frame. The loading was done to ensure that the test specimen will be subjected to concentric load only. Simple supports in the form of ball-and socket system were attached to the end of the members during compressions tests to let the whole length of the member be effective. Picture of the experimental setup is shown in Figure 2.



Fig. 2. Concentric compression loading of specimen showing buckling failure

Three failure modes were considered for the CFS members in concentric compression. They are full yielding, torsional or flexural-torsional buckling and distortional buckling. Full yielding is the failure when of the stress in whole cross section reach yield stress. Torsional or flexural torsional buckling is due to the lateral displacement that occurs, creating twisting and bending of the member. Distortional failure happens when the flanges rotate about the web junction displacing the flange from its original position. In addition, the effectiveness of the elements of the section was taken into account. With the effect of local buckling on the section, the widths of each element was reduced thus resulting to a

lesser cross sectional area than the full area. Formulas found in NSCP Sections 552 and 553 were used.

3. RESULTS AND DISCUSSION

The compressive strength values from the experimental and computational results were compared. The experiments and computations were group into different cases according to the CFS specimens' thicknesses and lengths. The failure modes observed in the experiments were carefully monitored.

Table 1. Failure modes

| Sample Code | Thick-ness | Length | Exp. Failure | Comp. Failure | Similar ? |
|-------------|------------|--------|--------------|---------------|-----------|
| A1 | 0.4 | 0.8 | DB | DB | Yes |
| B1 | 0.5 | 0.8 | DB | DB | Yes |
| C1 | 0.6 | 0.8 | DB | DB | Yes |
| D1 | 0.8 | 0.8 | DB | DB | Yes |
| E1 | 1.0 | 0.8 | DB | DB | Yes |
| A2 | 0.4 | 1.1 | DB | DB | Yes |
| B2 | 0.5 | 1.1 | DB | DB | Yes |
| C2 | 0.6 | 1.1 | DB | DB | Yes |
| D2 | 0.8 | 1.1 | TF | DB | No |
| A3 | 0.4 | 1.4 | DB | DB | Yes |
| B3 | 0.5 | 1.4 | TF | DB | No |
| C3 | 0.6 | 1.4 | TF | DB | No |
| D3 | 0.8 | 1.4 | TF | DB | No |
| B4 | 0.5 | 1.8 | TF | DB | No |
| D4 | 0.8 | 1.8 | TF | DB | No |
| E4 | 1.0 | 1.8 | TF | DB | No |
| A5 | 0.4 | 2.0 | TF | DB | No |
| B5 | 0.5 | 2.0 | TF | DB | No |
| C5 | 0.6 | 2.0 | TF | TF | Yes |
| D5 | 0.8 | 2.0 | TF | DB | No |
| C0 | 0.6 | 1.7 | TF | DB | No |
| D0 | 0.8 | 1.7 | TF | DB | No |

Displayed in Table 1 are the failure modes for each sample classification. It is divided into two, the failure mode in the experiment and the failure mode in the computation. Distortional Buckling failure is denoted as DB while Torsional Flexural Buckling failure is denoted as TF. Experimentally, DB happened for lengths of 0.8 meters and 1.1 meters except for samples in D2 which had length of 1.1 m with thickness of 0.8 mm. TF occurred for

lengths of 1.4, 1.7, 1.8, 2.0 meters except for samples in A3 which had length of 1.4 m and thickness of 0.4 mm. In terms of the computation, all samples are predicted to fail in the DB mode except for one sample category which is C5. None of the samples failed in yielding. It is observed that the experimental failure modes were not all predicted correctly by the computational method specified in the NSCP. However, all samples experimentally failed in DB were predicted correctly by computation. But, TF in the experiment was not predicted computationally except for samples of C5.

Table 2. Compressive strength results

| Sample Code | Actual Failure | Ave. Expt. Result | Ave. Comp. Result | Ratio |
|-------------|----------------|-------------------|-------------------|-------|
| A1 | DB | 1.86 | 0.89 | 2.10 |
| B1 | DB | 3.74 | 1.62 | 2.31 |
| C1 | DB | 5.08 | 1.77 | 2.88 |
| D1 | DB | 6.86 | 2.03 | 3.38 |
| E1 | DB | 10.06 | 3.25 | 3.09 |
| A2 | DB | 3.18 | 1.02 | 3.12 |
| B2 | DB | 6.68 | 1.41 | 4.75 |
| C2 | DB | 7.60 | 1.84 | 4.13 |
| D2 | TF | 10.42 | 4.17 | 2.50 |
| A3 | DB | 3.38 | 1.04 | 3.24 |
| B3 | TF | 5.48 | 2.17 | 2.52 |
| C3 | TF | 6.18 | 2.48 | 2.50 |
| D3 | TF | 9.10 | 3.45 | 2.64 |
| B4 | TF | 2.55 | 1.60 | 1.60 |
| D4 | TF | 4.76 | 2.59 | 1.84 |
| E4 | TF | 9.18 | 3.75 | 2.45 |
| A5 | TF | 1.23 | 0.88 | 1.41 |
| B5 | TF | 2.46 | 1.38 | 1.79 |
| C5 | TF | 2.50 | 1.72 | 1.45 |
| D5 | TF | 3.50 | 2.23 | 1.57 |
| C0 | TF | 3.53 | 2.05 | 1.73 |
| D0 | TF | 6.53 | 2.72 | 2.40 |

To verify the accuracy of the values of actual and theoretical compressive strength, the actual failure mode was followed and compared to its corresponding theoretical failure mode. Table 2 tabulates the corresponding values experimentally

and computationally obtained for each sample group. The ratio of experimental value against the computational value describes the variance of values.

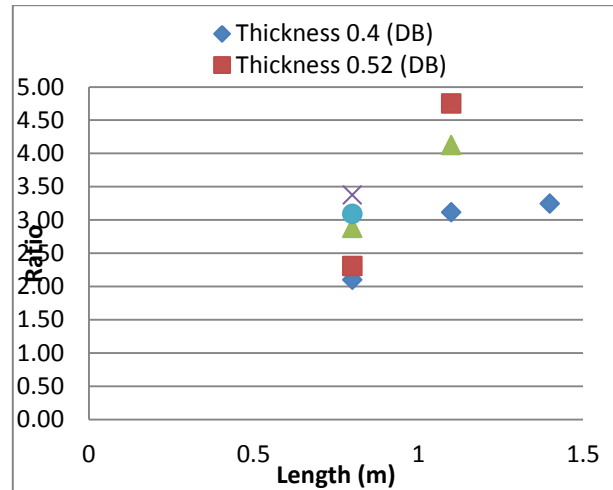


Fig. 3. Strength ratios for distortional buckling

Figure 3 shows the ratio of experimental compressive strength against the computational compressive strength for all samples with distortional buckling failure obtained experimentally. The largest ratio is 4.75 for samples of thickness 0.5 mm and length 1.1 m. This depicts an actual compressive strength of almost five times the computed value. The lowest ratio is 2.10 for samples of the thinnest thickness of 0.4 mm and shortest length of 0.8 m. Even for the lowest difference, the magnitude of deviation is more than twice the computed value. For the thicknesses with two or more lengths failing in distortional buckling, 0.4 mm, 0.5 mm and 0.6 mm, the increase in length contributes to the increase of difference of the experimental compressive strength and computational compressive strength. The ratio of a thickness of 0.6 mm from length of 0.8 m to 1.1 m increases in value. For the lengths with 2 or more thicknesses failing in distortional buckling, the ratio does not exhibit a definite increase or decrease of ratio. The ratio for length of 1.1 m with 0.8 mm thickness is larger than the ratio for of the same length but with a thickness of 1.0 mm. But it is higher than the ratio of the same length but with a thinner thickness of 0.5 mm.

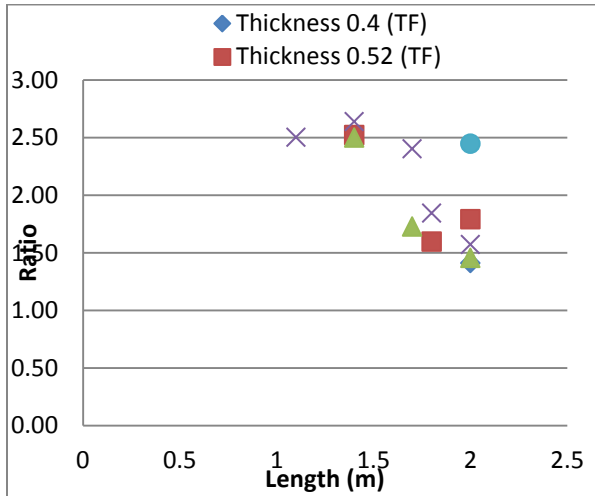


Fig. 4. Strength ratios for torsional-flexural buckling

Figure 4 shows the ratio of experimental compressive strength with respect to the computational compressive strength for all samples with torsional-flexural buckling failure obtained experimentally. The largest ratio is 2.64 for samples with thickness of 0.8 mm and length 1.4 m. The lowest ratio is 1.41 for samples with the thinnest thickness of 0.4 mm and longest length of 2.0 mm. As the length increases, the ratio does not have a general behavioural pattern that can be established. For the thickness 0.8 mm, from a length of 0.8 m to 1.1 m, the ratio increased. But from length of 1.1 m to length of 2.0 m, the ratio decreased. For thickness of 0.6 mm, the ratio decreases as the length increases. For thickness of 0.5 mm, it decreases then increased from 1.4 m to 1.7 m and 1.7 m to 2.0 m respectively. Similarly, the change in thickness for the same length does not show a behavioural pattern that can be generalized for the increase or decrease of ratio. For the length of 2.0 m, the ratio for thickness of 0.5 mm is greater than that for thickness of 0.8 mm but lower than thickness of 1.0 mm.

Plotted in Figure 5 are the experimental strength values versus the corresponding computational strength values. In the middle of the figure, a straight line is drawn to show the division between two areas. Any points lying on the line pertains to equal computational value and experimental value. Failures are color-coded into two to distinguish distortional buckling and torsional-buckling failures. All of the points plotted on the

graph are above the line of equality. This means that experimental values are higher than the computational values. For both distortional buckling and torsional flexural buckling, the computed strength values are conservative being greater than the experiment strength results. In addition, distortional buckling failures are even more conservative than the torsional buckling failures. All of the points of the distortional buckling failure are higher and greater than the torsional flexural buckling failure. Another observation is as the strength values increases, the points grow farther from the line of equality and thus make it more conservative. This occurs for both types of failure.

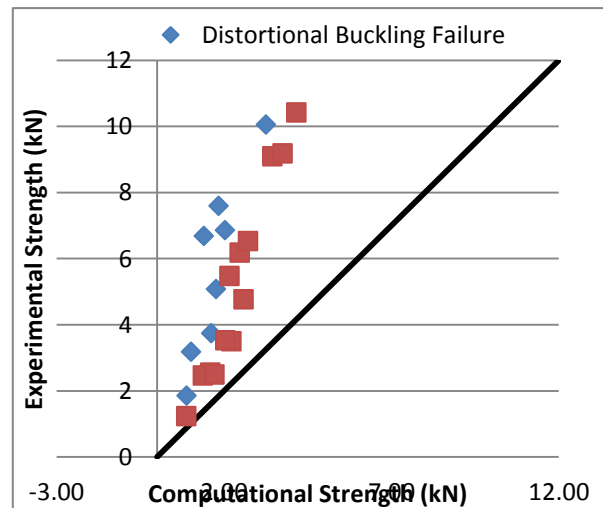


Fig. 5. Experimental versus computation strength

4. CONCLUSIONS

This study was conducted experimentally and computationally to evaluate the compressive strength of cold-formed steel channels with one section configuration but with varying thicknesses and lengths. For the computational method, the provisions found in the NSCP for cold-formed steel columns were used for calculation of the strength. An experimental setup accompanied in the attainment of the actual compressive strength of the samples.

It is found, through the computational method, that the buckling stress of the samples decrease as the length increases but is otherwise for



the effective area of the samples. The interaction of global and local buckling then exhibits differently with relation to the change in length. Failure of the samples in the experiment were divided into two, distortional buckling and torsional-flexural buckling. Sample groups with shorter lengths, specifically lengths of 0.8 m and 1.1 m, failed in distortional buckling. Sample groups with longer lengths on the other hand failed mostly on torsional-flexural buckling. For the computational method, all of the sample groups were predicted to fail on distortional buckling except for one sample group.

The consistency of failures predicted by the computations and the actual failure in experiment is very low. Less than half of the sample groups had correct failure mode predictions. Most of correct predictions are for distortional buckling and only one for torsional-flexural buckling. The other actual torsional-flexural buckling failures were not predicted correctly by the computational method.

The comparison of the compressive strength values for the sample groups displayed very conservative and low predictions as to the actual compressive strength values. Distortional buckling failures have in general very low predictions resulting to having an actual strength of almost five times the predicted value. The nearest prediction for the actual strength was more than twice the predicted value. Sample groups with torsional-flexural buckling failures had nearer predictions. The highest variation of the results is an actual value of having twice and a half than the predicted value. The lowest variation of actual value to predicted value is with only an increase of half of the predicted value. Torsional-flexural buckling computations are more accurate than distortional buckling failure predictions.

Thus, the provisions found in the NSCP for compression cold-formed steel members do not produce accurate strength predictions of actual cold-formed channel members. The provisions must be modified and adjusted to predict the compressive strength of the cold formed steel members manufactured in the Philippines. However, the cold-formed steel members performed well above the predictions. The actual strength is higher for strength designs using the current NSCP provisions.

5. ACKNOWLEDGMENTS

The authors are greatly indebted to several people who helped in the success of this study. Special acknowledgement is due to the following: (1) The faculty and staff of the Civil Engineering Department of De La Salle University, (2) ERDT for providing scholarship and study grant and (3) NedSteel Light Gage Steel Company for providing the materials for the experiment and ample information on their projects.

6. REFERENCES

- Chou, S. M., Seah, L. K., & Rhodes, J. (1996). The accuracy of some codes of practice in predicting the load capacity of cold-formed columns. *Journal of Constructional Steel Research*, 37(2), 137–172. doi:10.1016/0143-974X(95)00021-M
- Davies, J. . (2000). Recent research advances in cold-formed steel structures. *Journal of Constructional Steel Research*, 55(1-3), 267–288. doi:10.1016/S0143-974X(99)00089-9
- Hancock, G., Murray, T., & Ellifritt, D. (2001). *Cold Formed Steel Structure to the AISI Specification*. Marcel Dekker Inc.
- Kwon, Y. B., Kim, B. S., & Hancock, G. J. (2009). Compression tests of high strength cold-formed steel channels with buckling interaction. *Journal of Constructional Steel Research*, 65(2), 278–289. doi:10.1016/j.jcsr.2008.07.005
- Lin, S.-H., Yu, W.-W., Galambos, T. V., & Wang, E. (2005). Revised ASCE specification for the design of cold-formed stainless steel structural members. *Engineering Structures*, 27(9), 1365–1372. doi:10.1016/j.engstruct.2005.03.007
- Loughlan, J., Yidris, N., & Jones, K. (2012). The failure of thin-walled lipped channel compression members due to coupled local-distortional interactions and material yielding. *Thin-Walled Structures*, 6, 14–21.



- Lue, D. M., Chung, P.-T., Liu, J.-L., & Pan, C.-L. (2009). Compressive Strength of Slender C- Shaped Cold-Formed Steel Members with Web Openings. *International Journal of Steel Structures*, *9*(3), 231–240.
- Meiyalagan, M., Anbarasu, M., & Sukumar, S. (2010). Investigation on Cold formed C section Long Column with Intermediate Stiffener & Corner Lips – Under Axial Compression. *International Journal of Applied Engineering Research, Dindigul*, *1*(1), 28–41.
- Narayanan, S., & Mahendran, M. (2003). Ultimate capacity of innovative cold-formed steel columns. *Journal of Constructional Steel Research*, *59*(4), 489–508. doi:10.1016/S0143-974X(02)00039-1
- Rondal, J. (2000). Cold formed steel members and structures General Report, *55*, 155–158.
- Schafer, B. W. (n.d.). *Thin-Walled Column Design Considering Local, Distortional and Euler Buckling*.
- Tian, Y. S., & Lu, T. J. (2004). Minimum weight of cold-formed steel sections under compression. *Thin-Walled Structures*, *42*(4), 515–532. doi:10.1016/j.tws.2003.12.011
- Young, B. (n.d.). Local Buckling and Shift of Effective Centroid of Slender Sections, 119–132.
- Young, B., & Rasmussen, K. J. R. (2006). Behaviour of cold-formed singly symmetric columns, *33*(1999), 83–102.
- Yu, W. (2000). *Cold-Formed Steel Design* (3rd ed.). John Wiley & Sons Inc.